International Journal of
Intelligent Systems and
Applications in Engineering
ISSN:2147-6799 www.atscience.org/IJISAE
Advanced Technology and Science
Original Research Paper

Neural Boundary Conditions in Optic Guides

Pınar ÖZKAN BAKBAK

Accepted 23th February 2015 DOI: 10.18201/ijisae.04354

Abstract: In this study, the boundary coefficients of Transverse Electric (TE) and Transverse Magnetic (TM) modes at a planar slab optic guides are modeled by Neural Networks (NN). After modal analysis, train and test files are prepared for NN. Multi-Layer Perceptron (MLP) and Radial Basis Function (RBF) neural networks are performed and compared with each other. NNs are expected to be capable of modeling optical fiber technology in industry as a result of this study.

Keywords: *Boundary Conditions, Optic Guides, Neural Network.*

1. Introduction

Optic fiber which is the main structure of optical system is preferred because of their small losses and high channel capacity. Optical system can work in conformity with the existing systems, and optic fiber is not influenced by electromagnetic fields [1-3].
In this study, neural networks (NN) are employed in optic guides for boundary conditions. An NN, also called artificial neural network (ANN), is a mathematical and computational model. The smallest unit of NN is an artificial neuron which is inspired by biological neural. In general all NNs are used to model complex relationships between input and output data. NNs can learn and generalize from existing data even required formulas and parameters are unavailable. Generalization, nonlinearity, adaptability of NN provide usage and easiness in all fields of science [6-8]. NN applications in the optical communication is ever-growing. In this study, Multi-Layer Perceptron (MLP) and Radial Basis Function (RBF) neural networks are used and compared for guided Transverse Electric (TE) and Transverse Magnetic (TM) modes through planar slab optic guides. Analytical results and network outputs are evaluated to find out about the usage of NN in optical fiber technology.
There are many NN applications in various areas and also optical technology. NNs have been successfully used in optical fiber technology for prediction, calibration, sensing parameters, etc. NN in [9] use fiber optic vibration sensing to predict the size and location of delamination in composite beams. On the other hand, the study in [10] describes NN based prediction of the response of a fiber optic sensor using evanescent field absorption. Moreover, intelligent statistical mode sensors are proposed and analyzed using several statistical features in [11] using NN.
The remainder of this paper is organized as follows: In the second part of the study, TE and TM modes are studied associated with modal analysis. TE and TM modes are determined by using the Maxwell equations, Helmholtz equations and dielectric-dielectric boundary conditions. TE and TM coefficients are found by equating the tangential components due to the nature of the boundary conditions. In the third part NN model is designed and indicated the inputs, outputs for our application. The study is concluded in section four by comparing analytical results and NN outputs.

Yildiz Technical University, Department of Electronic and Communication Engineering, Davutpasa, 34220, Istanbul, Turkey
pozkan@yildiz.edu.tr

2. Modal Analysis in Planar Slab Optic Guides

Modal analysis of TE and TM modes is determined by using the Maxwell equations, Helmholtz equations and dielectric-dielectric boundary conditions. Additionally, electrical properties of the optic medium and the law of the light reflection-refraction are important to examine the guided modes. The refractive index of the core must be greater than the refractive index of the surrounding area in order to keep the light in the core [1-5, 12, 13].
Figure1 shows a planar slab optic guide extending to infinity in the y direction with diameter 2d. Electromagnetic properties showed no change in the y direction. In this case the mathematical arrangements must be with the Eq. (1).

$$\frac{\partial}{\partial y} \equiv 0 \tag{1}$$

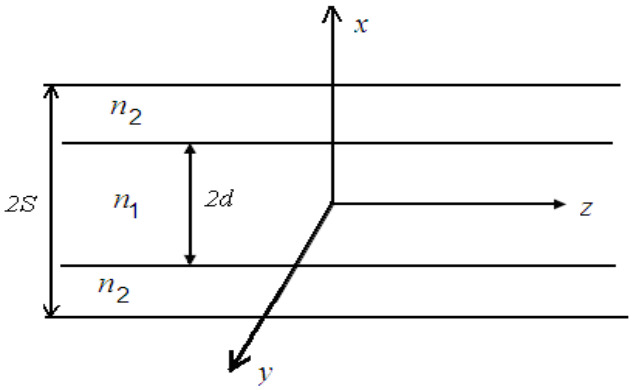

Figure1: Cladded planar slab optic fibers

A guided optic wave propagates in the guide along its longitudinal direction. We consider a straight guide whose longitudinal direction is taken to be in the z direction. Therefore, the electric and magnetic fields are:

$$\vec{E} = \vec{E}_0(x,y)\exp[\,j(\omega t - \beta z)]) \tag{2}$$

$$\vec{H} = \vec{H}_0(x,y)\exp[\,j(\omega t - \beta z)]) \tag{3}$$

Ampère and Faraday rules are given in optic guides by

$$\vec{\nabla}\times\vec{H} = j\omega\varepsilon\ \vec{E} \tag{4}$$

$$\vec{\nabla}\times\vec{E} = -j\omega\mu\ \vec{H} \tag{5}$$

By substituting Eq. (2) and Eq. (3) into Eq. (4) and Eq. (5), the field components are obtained as follows:

$$E_x = -\frac{j}{\kappa^2}\left(\beta\frac{\partial E_z}{\partial x} + \omega\mu\frac{\partial H_z}{\partial y}\right) \tag{6}$$

$$E_y = -\frac{j}{\kappa^2}\left(\beta\frac{\partial E_z}{\partial y} - \omega\mu\frac{\partial H_z}{\partial x}\right) \tag{7}$$

$$H_x = -\frac{j}{\kappa^2}\left(\beta\frac{\partial H_z}{\partial x} - \omega\varepsilon\frac{\partial E_z}{\partial y}\right) \tag{8}$$

$$H_y = -\frac{j}{\kappa^2}\left(\beta\frac{\partial H_z}{\partial y} + \omega\varepsilon\frac{\partial E_z}{\partial x}\right) \tag{9}$$

κ is the core region eigenvalue, where

$$\kappa^2 = k_1^2 - \beta^2 = (n_1 k_0)^2 - \beta^2 = \omega^2\mu_0\varepsilon_1 - \beta^2 \tag{10}$$

and β is the phase constant and also propagation constant in optic guides.

The components in the z direction are the longitudinal field components and the others are transverse field components. Transverse component will be found by finding the longitudinal ones. Therefore Helmholtz equation is used that is valid in homogeneous media with no source as follows:

$$\frac{\partial^2 E_z}{\partial x^2} + \frac{\partial^2 E_z}{\partial y^2} + \frac{\partial^2 E_z}{\partial z^2} + k^2 E_z = 0 \tag{11}$$

$$\frac{\partial^2 E_z}{\partial x^2} + \frac{\partial^2 E_z}{\partial y^2} + \kappa^2 E_z = 0 \tag{12}$$

$$\frac{\partial^2 H_z}{\partial x^2} + \frac{\partial^2 H_z}{\partial y^2} + \kappa^2 H_z = 0 \tag{13}$$

TE and TM mode solutions are divided into two part as periodic even modes and periodic odd modes. The modes attenuates exponentially in the region surrounding the core.

Rearranging the Eq.s (6), (7), (8), (9) with the Eq.(1),

$$E_x = -\frac{j}{\kappa^2}\left(\beta\frac{\partial E_z}{\partial x}\right) \tag{14}$$

$$E_y = \frac{j}{\kappa^2}\left(\omega\mu\frac{\partial H_z}{\partial x}\right) \tag{15}$$

$$H_x = -\frac{j}{\kappa^2}\left(\beta\frac{\partial H_z}{\partial x}\right) \tag{16}$$

$$H_y = -\frac{j}{\kappa^2}\left(\omega\varepsilon\frac{\partial E_z}{\partial x}\right) \tag{17}$$

Thus the transverse components are expressed in terms of longitudinal components in the planar slab optic guides.

2.1. TE and TM modes in Planar Slab Optic Guides

2.1.1. TE modes

The electric field component in the propagation direction $Ez = 0$. Thus, Ey, Hx and Hz components are available. The Helmholtz equation

$$\frac{\partial^2 E_y}{\partial x^2} + \kappa^2 E_y = 0 \tag{18}$$

with the Ey field component

$$H_x = -\frac{\beta}{\omega\mu_0}E_y \tag{19}$$

$$H_z = \frac{j}{\omega\mu_0}\frac{\partial E_y}{\partial x} \tag{20}$$

Eq. (18) gives different solutions in the core and clad regions. Because the electric field propagates differently in the core and the clad.

2.1.1.1. Guided Even TE modes

In the core region $|x| \le d$,Ey field component is found from the solution of Eq.(18) that

$$E_{y1} = A_1\cos(\kappa x) \tag{21}$$

With Ey, the magnetic fields are as follows:

$$H_{x1} = -\frac{\beta}{\omega\mu_0} A_1 \cos(\kappa x) \quad (22)$$

$$H_{z1} = \frac{j\kappa}{\omega\mu_0} A_1 \sin(\kappa x) \quad (23)$$

In the clad region ($|x| \geq d$) electric and magnetic fields are given by

$$E_{y2} = A_2 \exp(-\gamma(|x| - d)) \quad (24)$$

$$H_{x2} = -\frac{\beta}{\omega\mu_0} A_2 \exp(-\gamma(|x| - d)) \quad (25)$$

$$H_{z2} = \frac{j\gamma}{\omega\mu_0}\left(\frac{-x}{|x|}\right) A_2 \exp(-\gamma(|x| - d)) \quad (26)$$

and γ is the clad region eigenvalue, where

$$\gamma^2 = \beta^2 - k_2^2 = \beta^2 - (n_2 k_0)^2 = \beta^2 - \omega^2 \mu_0 \varepsilon_2 \quad (27$$

Dielectric-dielectric boundary conditions required by the equation of the field tangential components at the border ($|x| = d$) as:

$$E_{y1} = E_{y2} \quad (28)$$

$$H_{z1} = H_{z2} \quad (29)$$

Pz is the power of the guided mode and A_1 can be obtained by Poynting's theorem as follows:

$$A_1 = \left(\frac{2\omega\mu_0\gamma}{\beta(1+\gamma d)} P_z\right)^{1/2} \quad (30)$$

Here it is possible to get A_2 by the help of boundary conditions.

$$A_2 = A_1 \cos(\kappa d) \quad (31)$$

2.1.1.2. Guided Odd TE modes

The field components in the core region ($|x| \leq d$) are obtained as follows:

$$E_{y1} = B_1 \sin(\kappa x) \quad (32)$$

$$H_{x1} = -\frac{\beta}{\omega\mu_0} B_1 \sin(\kappa x) \quad (33)$$

$$H_{z1} = \frac{j\kappa}{\omega\mu_0} B_1 \cos(\kappa x) \quad (34)$$

In the clad region ($|x| \geq d$) electric and magnetic fields are given by

$$E_{y2} = B_2 \exp(-\gamma(|x| - d)) \quad (35)$$

$$H_{x2} = -\frac{\beta}{\omega\mu_0} B_2 \exp(-\gamma(|x| - d)) \quad (36)$$

$$H_{z2} = \frac{j\gamma}{\omega\mu_0}\left(\frac{-x}{|x|}\right) B_2 \exp(-\gamma(|x| - d)) \quad (37)$$

The field tangential components are equal at the border required by the dielectric-dielectric boundary conditions as:

$$E_{y1} = E_{y2} \quad (38)$$

$$H_{z1} = H_{z2} \quad (39)$$

It is possible to find the odd TE mode coefficient in the core by Poynting's theorem and in the clad by Boundary conditions as follows:

$$B_1 = \left(\frac{2\omega\mu_0\gamma}{\beta(1+\gamma d)} P_z\right)^{1/2} \quad (40)$$

$$B_2 = B_1 \sin(\kappa d) \quad (41)$$

2.1.2. TM Modes

The magnetic field component in the propagation direction $Hz = 0$. Thus Ex, Ez and Hy components are available. The Helmholtz equation is given by

$$\frac{\partial^2 H_y}{\partial x^2} + \kappa^2 H_y = 0 \quad (42)$$

With the Hy field component, the electric fields are as follows:

$$E_x = \frac{\beta}{\omega\varepsilon} H_y \quad (43)$$

$$E_z = -\frac{j}{\omega\varepsilon}\frac{\partial H_y}{\partial x} \quad (44)$$

2.1.2.1. Guided Even TM modes

In the core region ($|x| \leq d$);

$$H_{y1} = C_1 \cos(\kappa x) \tag{45}$$

In the clad region ($|x| \geq d$)

$$H_{y2} = C_2 \exp(-\gamma(|x| - d)) \tag{46}$$

C_1 can be obtained by Poynting's theorem .

$$C_1 = \left(\frac{2\omega\varepsilon_0 n_1^2 P_z}{\beta\left[d + \frac{n_1^2 n_2^2}{\gamma} \frac{\kappa^2 + \gamma^2}{n_2^4\kappa^2 + n_1^4\gamma^2} \right]} \right)^{1/2} \tag{47}$$

TM mode coefficient is found by Boundary conditions in the clad region as follows:

$$C_2 = C_1 \cos(\kappa d) \tag{48}$$

2.1.2.2. Guided Odd TM modes

In the core region ($|x| \leq d$);

$$H_{y1} = D_1 \sin(\kappa x) \tag{49}$$

In the clad region ($|x| \geq d$)

$$H_{y2} = D_2 \exp(-\gamma(|x| - d)) \tag{50}$$

D_1 can be obtained by Poynting's theorem.

$$D_1 = \left(\frac{2\omega\varepsilon_0 n_1^2 P_z}{\beta\left[d + \frac{n_1^2 n_2^2}{\gamma} \frac{\kappa^2 + \gamma^2}{n_2^4\kappa^2 + n_1^4\gamma^2} \right]} \right)^{1/2} \tag{51}$$

It is possible to find the odd TM mode coefficient in the clad by Boundary conditions.

$$D_2 = D_1 \sin(\kappa d) \tag{52}$$

3. Neural Network Design

3.1. Multilayer Perceptron (MLP)

MLP networks contain successive linear transformations followed by processing with nonlinear activation functions. They also implement nonlinear transformations for function approximation. The network consists of input layer, hidden layers and output layer. Every layer computes the activation function of a weighted sum of the layer's inputs.

Some issues which must be regarded in designing and training a MLP :

- The number of hidden layers
- The number of neurons in each hidden layer
- A globally optimal solution that avoids local minimum
- An optimal solution in a reasonable period of time.

3.2. Radial Basis Function (RBF)

RBF network is a feed-forward neural network using radial basis functions. The input layer is made up source nodes. The second layer is hidden layer. The output layer supplies the response of the network to the activation patterns applied to the input layer.

Given the inputs xj, the total input to the ith hidden neuron γi is given by

$$\gamma_i = \sqrt{\sum_{j=1}^{n} \left(\frac{x_j - c_{ij}}{\lambda_{ij}} \right)^2} \tag{53}$$

for $i = 1, 2, \ldots, N$, where, N is the number of hidden neurons. The output value of the ith hidden neuron is $zij = \sigma(\gamma i)$, where $\sigma(\gamma)$ is a radial basis function. The outputs of the RBF network are computed from hidden neurons as

$$y_k = \sum_{i=1}^{N} w_{ki} z_{ki} \tag{54}$$

where, wki is the weight of the link between the ith neuron of the hidden layer and the kth neuron of the output layer. Training parameters of the RBF network consist of wki, cij , and λij for $k = 1, 2, \ldots, m, i = 1, 2, \ldots., N,$ and $j = 1, 2, \ldots n$ [11].

3.3. Methods and Simulations

In our work NNs designed for boundary coefficients in optic guides consist of 5 inputs and 4 outputs. Both MLP and RBF were trained with 50 samples and tested with 50 samples determined according to the definition of the problem. The training and test data of NN were obtained from formula results given in section 2.

The input and output parameters are defined as follows:

The input parameters are

- $n1$ and $n2$: refractive indexes of core and clad
- d : radius of the core
- β :phase constant
- f :working frequency,

and the output parameters are

- real and imaginary part of A_1
- real and imaginary part of C_1.

The MLP network, which has a configuration of 5 input neurons, 1 hidden layer with 10 neurons and 2 output neurons with learning rate = 0.6, goal = 10^{-9}, is trained for1000 epochs. In the RBF network, the spread value is chosen as 0.7, which gives the best accuracy. The results consisting of target and neural network outputs are shown in Table 1, 2 and 3 respectively. Table 4 shows the performance of MLP and RBF.

4. Conclusion

In this work, the neural network is employed as a toll in design of optic fibers for boundary conditions. MLP and RBF neural network outputs have shown good accuracy from available data without processing long and complex equations. Using NN in optical fiber technology gives an advantage when formulas and parameters are unavailable, nonlinear, long or complex. NN can be applied to other fields of optical communications.

Table 1: Normalized target values from analytical results

Normalized test values from analytical results			
Real{*A1*}	Imag{*A1*}	Real{*C1*}	Imag{*C1*}
0,98027	0,86815	0,43701	0,65630
0,85098	0,59347	0,37221	0,44177
0,68318	0,32248	0,29305	0,23608
0,91904	0,64459	0,51645	0,59846
0,73240	0,29364	0,52469	0,34163
0,77968	0,45111	0,39669	0,38350
0,68327	0,31853	0,29350	0,23345
0,78195	0,36222	0,44708	0,34372
0,74594	0,39702	0,33094	0,29954
0,66652	0,25432	0,32251	0,20777
0,67616	0,35627	0,29597	0,26624
0,95620	0,77225	0,48037	0,64950
0,71040	0,29141	0,3974	0,26990
0,98335	0,79536	0,56115	0,74822
0,74309	0,49399	0,33168	0,37424

Table 2: MLP neural network output values

MLP neural network outputs			
Real{*A1*}	Imag{*A1*}	Real{*C1*}	Imag{*C1*}
0,98002	0,86835	0,43690	0,65622
0,85149	0,59412	0,37213	0,44192
0,68299	0,32273	0,29381	0,23716
0,91880	0,64424	0,51632	0,59724
0,73181	0,29629	0,52577	0,34224
0,77990	0,45085	0,39691	0,38314
0,68305	0,31874	0,29424	0,23445
0,78330	0,36084	0,44760	0,34766
0,74624	0,39657	0,33098	0,30024
0,66562	0,25278	0,32249	0,2068
0,67609	0,35757	0,29626	0,26600
0,95593	0,77338	0,48030	0,64927
0,71048	0,29110	0,39738	0,26956
0,98438	0,79492	0,56162	0,74913
0,74303	0,49369	0,33152	0,37410

Table 3: RBF neural network output values

RBF neural network outputs			
Real{*A1*}	Imag{*A1*}	Real{*C1*}	Imag{*C1*}
0,98048	0,86910	0,43719	0,65782
0,85088	0,59388	0,37218	0,44235
0,68314	0,32265	0,29301	0,23617
0,91937	0,64445	0,51683	0,59927
0,73264	0,29525	0,52452	0,34197
0,77960	0,45056	0,39667	0,38320
0,68321	0,31855	0,29345	0,23339
0,78113	0,36197	0,44670	0,34501
0,74612	0,39952	0,33107	0,3018
0,66687	0,25274	0,32275	0,20773
0,67635	0,35268	0,29623	0,26408
0,95647	0,77455	0,48059	0,65190
0,71015	0,28701	0,39737	0,26708
0,98304	0,79456	0,56075	0,74607
0,74303	0,49448	0,33161	0,37411

Table 4: Percentage accuracy performance of MLP and RBF

	%Accuracy
MLP	99.81
RBF	98.74

References

[1] D. Marcuse, Theory of Dielectric Optical Waveguides (Academic Press, New York, 1974).

[2] A.W. Snyder, J.D. Love, Optical Waveguide Theory (J.W. Arrowsmith, Bristol, 1983).

[3] J. M. Senior, Optical Fiber Communications (Second Edition, Prentice-Hall, Cambridge, 1992).

[4] A. H. Cherin, An Introduction to Optical Fibers, (Mcgraw Hill, New York, 1983.)

[5] G. Keiser, Optical Fiber Communications, (McGraw-Hill, New York, 1983.)

[6] J.M. Zurada, Introduction to Artificial Neural Systems (St. Paul, MN:West Publishing Company, 1992).

[7] R.J. Schalkoff, Artificial Neural Networks, (McGraw-Hill, Singarope, 1997).

[8] S. Haykin, Neural Networks: A Comprehensive Foundation (Newyork: Mcamillan and IEEE Computer Society, 1999).

[9] S.E. Watkins, G.W. Sanders, F. Akhavan and K. Chandrashekhara "Modal analysis using fiber optic sensors and neural networks for prediction of composite beam delamination", Smart Materials and Structures, 11, 489-495 (2002).

[10] O.G. Saracoglu,"An artificial neural network approach for the prediction of absorption measurements of an evanescent field fiber sensor", Sensors, 8, 1585-1594 (2008).

[11] H.S. Efendioglu, O. Toker,T. Yildirim, K. Fidanboylu, "Intelligent fiber optic statistical mode sensors using novel features and artificial neural networks", Proc. SPIE 8693, Smart Sensor Phenomena, Technology, Networks, and Systems Integration (2013).

[12] P. Ozkan Bakbak, Optical Coupler Design, MSc Thesis

(Yildiz Technical University 2008).
[13] N. O. Unverdi, Optik Fiberlerde Propagasyon Özelliklerinin İncelenmesi ve Bükülme Kaybının Analizi, Yüksek Lisans Tezi (Yıldız Teknik Üniversitesi, İstanbul, 1991)
[14] J.Park, W.I. Sandberg, "Universal Approximation Using Radial Basis Function Networks", Neural Computation, Vol. 3, pp. 246-257(1991).

